SPANDIDOS PUBLICATIONS

MOLECULAR MEDICINE REPORTS 27: 62, 2023

RCAS1 increases cell morphological changes in murine fibroblasts by reducing p38 phosphorylation

TAKUYA NISHINAKAGAWA*, MAI HAZEKAWA*, MASATO HOSOKAWA and DAISUKE ISHIBASHI

Department of Immunological and Molecular Pharmacology, Faculty of Pharmaceutical Science, Fukuoka University, Fukuoka 814-0180, Japan

Received February 5, 2022; Accepted December 9, 2022

DOI: 10.3892/mmr.2023.12949

Abstract. Receptor-binding cancer antigen expressed on SiSo cells (RCAS1) is a tumor-associated antigen that is expressed in a number of human malignancies. RCAS1 acts as a ligand for a putative RCAS1 receptor that is present on various human cells including T and B lymphocytes and natural killer cells, in which it induces cell growth inhibition and apoptosis. It has been suggested that RCAS1 might serve an important role in tumor cell evasion from the host immune system. In fact, RCAS1 expression is related to malignant characteristics including tumor size, invasion depth, clinical stage and poor overall survival. The authors previously established doxycycline-induced RCAS1 overexpression murine fibroblast L cells to analyze the biological functions of RCAS1 and reported that its expression inhibited cell cycle progression *via* the downregulation of cyclin D3, which subsequently induced apoptosis. Additionally, it was found that RCAS1 expression induced cell morphological changes prior to caspase-mediated apoptosis. Thus, the present study examined signaling pathways associated with changes in cell morphology that were induced by RCAS1 expression. The data showed that increased RCAS1 expression caused a reduction in actin stress fibers and decreased cofilin phosphorylation. Recent studies have shown that p38 signaling regulates actin polymerization. The data the present study showed that increased RCAS1 expression significantly decreased p38 phosphorylation.

Correspondence to: Dr Takuya Nishinakagawa or Professor Daisuke Ishibashi, Department of Immunological and Molecular Pharmacology, Faculty of Pharmaceutical Science, Fukuoka University, 8-19-1 Nanakuma, Jonan-ku, Fukuoka 814-0180, Japan
E-mail: tnishi0703@fukuoka-u.ac.jp
E-mail: dishi@fukuoka-u.ac.jp

*Contributed equally

Key words: receptor-binding cancer antigen expressed on SiSo cells, cell morphological change, actin dynamics, p38 MAP kinase

Introduction

Tumor cells use various mechanisms to escape from host anti-tumor immune responses, such as secreting TGF-β and IL-10. These cytokines are often detected at high levels in malignancies and affect immune cell proliferation, activation and differentiation (1-5). Another mechanism termed tumor counterattack involves the expression of apoptosis-related proteins by tumor cells also to suppress host anti-tumor immune responses. TNF-related apoptosis-inducing ligand (TRAIL) and Fas ligand (FasL/CD95L) are ligands of the TNF family that are associated with specific receptors of the TNF receptor superfamily and induce apoptosis (6). FasL overexpression is found in various human tumor cells and FasL binds to Fas-positive cytotoxic T lymphocytes (CTLs) (7-12). Additionally, several experiments have observed TRAIL-mediated apoptosis in activated CTLs that have infiltrated tumor tissue (13-16). Thus, FasL and TRAIL expression on tumor cells serve critical roles in inducing apoptosis in anti-tumor immune effector cells, allowing for escape from immune surveillance.

Receptor-binding cancer antigen expressed on SiSo cells (RCAS1) is a tumor-associated antigen expressed in various human carcinomas. Initially, the 22-1-1 monoclonal antibody (22-1-1 mAb) was raised against human uterine carcinoma cell line, SiSo cells (17,18). Then, a cDNA encoding the antigen recognized by 22-1-1 mAb was isolated and named RCAS1 (19). RCAS1 is detectable by immunohistochemistry and levels of soluble-form RCAS1 in human serum or cancer cell culture supernatant can be measured by enzyme-linked immunosorbent assay (ELISA) (20). A number of reports have shown the clinical significance of RCAS1 as a biomarker for the diagnosis and prognosis of malignant human tumors. RCAS1 expression has been observed in various malignant tumors and is correlated with poor prognosis of cancer patients; serum RCAS1 levels are also found to be significantly higher in cancer patients compared with healthy blood donors (21-25). Soluble-form RCAS1 has been shown to induce apoptosis in various human cell lines including normal peripheral lymphocytes, such as T and B cells and natural killer cells (19,26). Additionally, RCAS1 levels in various human malignancies are correlated with the number of apoptotic tumor infiltrating lymphocytes (TILs) surrounding the tumor cells (23,24). To investigate the biological functions of RCAS1, the authors

previously established a doxycycline (Dox)-induced RCAS1 overexpression model in murine fibroblast L cells (L/ind RCAS1) and reported that RCAS1 expression inhibited cell cycle progression *via* the downregulation of cyclin D3, which subsequently induced apoptosis in L/ind RCAS1 cells (27). Additionally, it was found that RCAS1 expression in L/ind RCAS1 cells induced morphological changes prior to caspase-mediated apoptosis. Several studies have shown that regulators of the actin cytoskeleton that are associated with migratory signals are increased in invasive and metastatic tumor cells (28-31). These results suggest that RCAS1 might not only be involved in a mechanism of tumor evasion from immune surveillance but could also serve a role in tumor cell invasion and migration.

The present study clarified the biological functions of RCAS1 by examining the signaling pathways associated with cell morphological changes that were induced by RCAS1 expression in L/ind RCAS1 cells, particularly those related to actin dynamics. Additionally, it is well known that the MAPK cascades serve critical regulatory roles in cell growth, differentiation, death and in controlling cellular responses to stress. Therefore, the present study also investigated the relationship between RCAS1 expression and MAPK signaling in L/ind RCAS1 cells.

Materials and methods

Cell lines and cell culture. To investigate the biological functions of RCAS1, a doxycycline (Dox)-induced RCAS1 overexpression model was established in murine fibroblast L cells (L/ind RCAS1) as described in a previous report (27). The present study used the human uterine cervical adenocarcinoma cell line SiSo and L/ind RCAS1 cells. These cells were cultured in Roswell Park Memorial Institute (RPMI) 1640 medium (Thermo Fisher Scientific, Inc.) supplemented with 10% heat-inactivated fetal bovine serum (Biowest), 100 nM non-essential amino acids (Nacalai Tesque, Inc.) and 1 mM sodium pyruvate (Nacalai Tesque, Inc.) at 37˚C in a 5% CO_2 atmosphere. To induce exogenous RCAS1 expression, doxycycline (Dox; FUJIFILM Wako Pure Chemical Corporation) was used. Dox was dissolved in dH_2O at 1 mg/ml concentration and L/ind RCAS1 cells were treated with 0.5 μg/ml Dox for the indicated times.

Preparation of SiSo cell culture supernatant containing soluble-form RCAS1. To collect the soluble-form RCAS1 from SiSo cell culture supernatant, SiSo cells were cultured in serum-free medium. Briefly, SiSo cells were cultured under normal conditions until reaching 80% confluency. Then, the cell culture medium was exchanged with fresh serum-free medium and the cells were cultured for 48 h. The cell culture supernatants were then collected and concentrated by ultrafiltration (Molecular weight cut-off >50 kDa). After dialysis to phosphate buffered saline (PBS), the obtained fractions were used in subsequent experiments as the SiSo supernatant (SiSo Sup/RCAS1$^+$).

ELISA. Soluble-form RCAS1 in SiSo Sup was measured by ELISA. Briefly, for precoating, 22-1-1 antibody (Medical & Biological Laboratories Co., Ltd.) was added to each well in a 96-well plate (100 μl/well) and incubated overnight at 4˚C. After washing with PBS, Blocking One solution (Nacalai Tesque, Inc.) was diluted 5-fold with PBS and added to each well for blocking. After 1 h of incubation at room temperature, diluted SiSo Sup was added and incubated for 1 h at room temperature. After washing, biotinylated 22-1-1 antibody was added and incubated for 1 h at room temperature. After washing, peroxidase-conjugated streptavidin (Thermo Fisher Scientific, Inc.) was added and incubated for 1 h at room temperature. Then, peroxidase substrate solution (TMB Microwell Peroxidase Substrate System Kirkegaard & Perry Laboratories, Inc.) was added to each well and incubated for 20 min at room temperature, followed by an equal volume of 1 M H_3PO_4. Absorbance was measured at 450 nm (reference wavelength: 655 nm) with a microplate reader (iMark Microplate Reader; Bio-Rad Laboratories, Inc.).

Immunodepletion of soluble-form RCAS1 from SiSo Sup. Immunodepletion of soluble-form RCAS1 from SiSo Sup (SiSo Sup/RCAS1$^-$) was performed by the following method. First, 22-1-1 antibody was used to prepare anti-RCAS1 beads by mixing 22-1-1 antibody and Pierce Protein L magnetic beads (Thermo Fisher Scientific, Inc.) and incubating overnight at 4˚C. After incubation, SiSo Sup was added to the solution containing antibody-Protein L complexes and incubated for 1 h at room temperature. After incubation, RCAS1-antibody-Protein L complexes were removed with a magnetic stand SiSo Sup/RCAS1$^-$ was collected. After immunodepletion, SiSo Sup/RCAS1$^-$ was used in ELISA.

Cytotoxicity of doxycycline to L cells. Cytotoxity test of Dox to L cells was performed by WST-8 assay. Cells (2.5×10^3) were seeded in a 96-well plate and incubated overnight at 4˚C. The culture medium was then replaced with fresh medium containing each concentration of Dox for 48 h. At the final 4-h, the cells were incubated with WST-8 reagent (FUJIFILM Wako Pure Chemical Corporation). Absorbance was measured using a iMark microplate reader (Bio-Rad Laboratories, Inc.) at 450 nm with a reference wavelength of 630 nm.

Time-lapse observation of cell morphological changes. L/ind RCAS1 cells (3×10^4) were seeded in a glass-bottom dish (Matsunami Glass Ind., Ltd.) and incubated overnight at 4˚C. After adding SiSo Sup or Dox, the cultured cells were observed by time-lapse imaging with a EVOS FL cell imaging system (Thermo Fisher Scientific, Inc.).

Confocal immunofluorescence microscopy. To observe actin stress fibers in L/ind RCAS1 cells, immunofluorescence staining was performed. L/ind RCAS1 cells (1×10^5) were seeded in a 35-mm poly-L-lysine coated glass-bottom dish and cultured for 48 h. After Dox induction, the cells were washed twice with cold PBS and fixed with 4% paraformaldehyde for 20 min at room temperature. The fixed cells were permeabilized with 0.1% Triton X-100 in PBS for 5 min at room temperature. After blocking with Blocking One solution (Nacalai Tesque, Inc.) for 1 h at room temperature, the cells were incubated with anti-RCAS1 antibody (ProteinTech Group, Inc.) in PBS overnight at 4˚C. After washing with PBS, the cells were incubated with fluorescein isothiocyanate (FITC)-conjugated goat-anti

mouse IgG (Beckman Coulter, Inc.) and 100 nM rhodamine phalloidin (Cytoskeleton, Inc.) for 2 h at room temperature. After washing with PBS, the stained cells were observed with a confocal microscope (LSM710; Zeiss AG).

Measurement of cell index by the real-time cell-monitoring analysis (RTCA) system. Cell index (CI) was acquired by the iCELLigence system (ACEA Biosciences, Inc.) as the RTCA system. All monitoring was performed at 37˚C with regulated CO_2 content (5%). E-plates (culture plates for the iCELLigence system) containing 100 μl culture medium per well were equilibrated to 37˚C and CI was set to zero under these conditions. L/ind RCAS1 cells ($2x10^4$ cells/well) were added in 50 μl culture medium. After 24 h incubation at 37˚C, Dox was added to each well. The CI was monitored in real-time for 48 h after cell seeding.

Analysis of the F-actin/G-actin ratio. Briefly, $1x10^5$ cells were seeded in a 35-mm dish and cultured for 48 h. After Dox induction, the cells were homogenized in 200 μl of F-actin stabilization buffer [50 mM PIPES (pH 6.9), 50 mM NaCl, 5 mM $MgCl_2$, 5 mM EGTA, 5% glycerol, 0.1% Triton X-100, 0.1% Nonidet P-40, 0.1% Tween-20, 0.1% 2-mercaptoethanol, 0.001% antifoam C, 1 mM ATP, 10 μM pepstatin A, 15 μM leupeptin, 10 mM benzamidine, 4 μM tosyl arginine methyl ester]. The supernatant of the protein extract was collected after centrifugation at 100,000 x g for 1 h at 37˚C. The pellet was resuspended in ice-cold distilled H_2O plus 10 μM cytochalasin D and then incubated on ice for 1 h to dissociate F-actin. The resuspended pellet was gently mixed every 15 min. Supernatant of the resuspended pellet was collected after centrifugation at 5,000 x g for 2 min at 4˚C. Equal volumes of the first (G-actin) and second (F-actin) supernatants were subjected to immunoblot analysis using anti-β-actin antibody (Merck KGaA).

Western blot analysis. Following Dox induction, L/ind RCAS1 cells were lysed in CelLytic-M (Merck) containing a protease inhibitor cocktail (Nacalai Tesque, Inc.) and phosphatase inhibitors (5 mM NaF, 1 mM Na_3VO_4). Cell lysates were centrifuged at 12,000 x g for 30 min at 4˚C and supernatants were collected. Protein concentrations of each sample were measured using the BCA protein assay kit (Thermo Fisher Scientific, Inc.). Equal amounts of protein (10 μg/lane) were electrophoresed on a 5-20% gradient SDS-Polyacrylamide gel electrophoresis (SDS-PAGE) gel and transferred onto PVDF membranes. The membranes were incubated with Blocking One solution (Nacalai Tesque, Inc.) containing phosphatase inhibitors for 1 h at room temperature, followed by incubation with the following primary antibodies for 1 h at room temperature: Anti-RCAS1 (cat. no. 66170-1; Proteintech Group, Ltd.; 1:5,000), anti-cofilin and anti-phosphorylated (p-) cofilin (cat. no. CK6040; ECM Biosciences; 1:2,000); anti-p38, anti-p-p38, anti-extracellular signal-regulated kinase (ERK) 1/2 and anti-p-ERK 1/2 (cat. nos. 9913 and 9926 Cell Signaling Technology, Inc.; 1:5,000). After washing with TBS -0.05% Tween, the membranes were incubated with peroxidase-conjugated goat anti-mouse IgG or peroxidase-conjugated goat anti-rabbit IgG (cat. nos. 7074 and 7076; Cell Signaling Technology, Inc.; 1:10,000) as secondary antibodies for 1 h at room temperature. Immunoreactive proteins were visualized using ImmunoStar LD (FUJIFILM Wako Pure Chemical Corporation). Images were captured using a Multi ImagerIIMultiBox (Bio Tools Inc.). Protein contents were compared with the corresponding GAPDH controls and normalized For quantification of blots, AlphaEaseFC Software (version 4.0.1; Alpha Innotech) was used.

Statistical analysis. All experiments were performed in triplicate and results are represented as mean ± standard deviation. Statistical significance was evaluated using one-way ANOVA followed by Tukey test. $P<0.05$ was considered to indicate a statistically significant difference.

Results

Cell morphological changes induced by soluble-form RCAS1. SiSo Sup/$RCAS1^+$ and SiSo Sup/$RCAS1^-$, which was the fraction that had soluble-form RCAS1 removed by immunodepletion, were prepared. The effect of soluble-form RCAS1 against wild-type L cells expressing the RCAS1 receptor was examined. After adding each SiSo Sup preparation ($RCAS1^+$/$RCAS1^-$) at a 1/100 v/v ratio, L cells were cultured for 24 h. Soluble-form RCAS1 in SiSo Sup/$RCAS1^+$ was detected by ELISA (Fig. 1A) and cell morphological changes (round shape) of L cells were observed after incubation with SiSo Sup/$RCAS1^+$ (Figs. 1B and S1). Conversely, RCAS1 was not detected in SiSo Sup/$RCAS1^-$ and the cell morphological changes were not induced (Fig. 1A and B). These results suggested that the cell morphological changes induced in L cells by SiSo Sup required RCAS1.

RCAS1 levels in L/ind RCAS1 cells and morphological changes. Previously it was found that RCAS1 expression induced cell morphological changes prior to caspase-mediated apoptosis in L/ind RCAS1 cells (27). To elucidate the mechanism of these cell morphological changes, L/ind RCAS1 cells were used to analyze the relationship between RCAS1 expression and cell morphological changes. L/ind RCAS1 cells, which transformed with a tetracycline induced *rcas1* gene expression system, were established previously (27). This cell line expressed RCAS1 protein by Dox induction. For this experiment, L/ind RCAS1 cells were treated with 0.5 μg/ml Dox over a course of time. The present study confirmed no cytotoxity at this concentration of Dox against L cells (Fig. S2). RCAS1 expression in L/ind RCAS1 cells was measured by western blotting using an anti-RCAS1 antibody. RCAS1 was detected at 4 h after Dox induction and increased in a time-dependent manner (Fig. 2A). After Dox stimulation, cell motility was initially decreased and a rounded morphology which is one of the characteristics of morphological changes in adherent cells was induced in contrast to the characteristic fibroblastic morphology of control cells (Dox -0 h; Fig. 2B). To further investigate the cell morphological changes induced by RCAS1 expression, the conformation of actin stress fibers in L/ind RCAS1 cells was examined by immunofluorescence using rhodamine phalloidin and anti-RCAS1 antibody. In control cells (Dox-0 h), actin stress fibers were spread throughout the cytosol. By contrast, the actin stress fibers had disappeared in RCAS1-expressing cells, which was correlated with increased

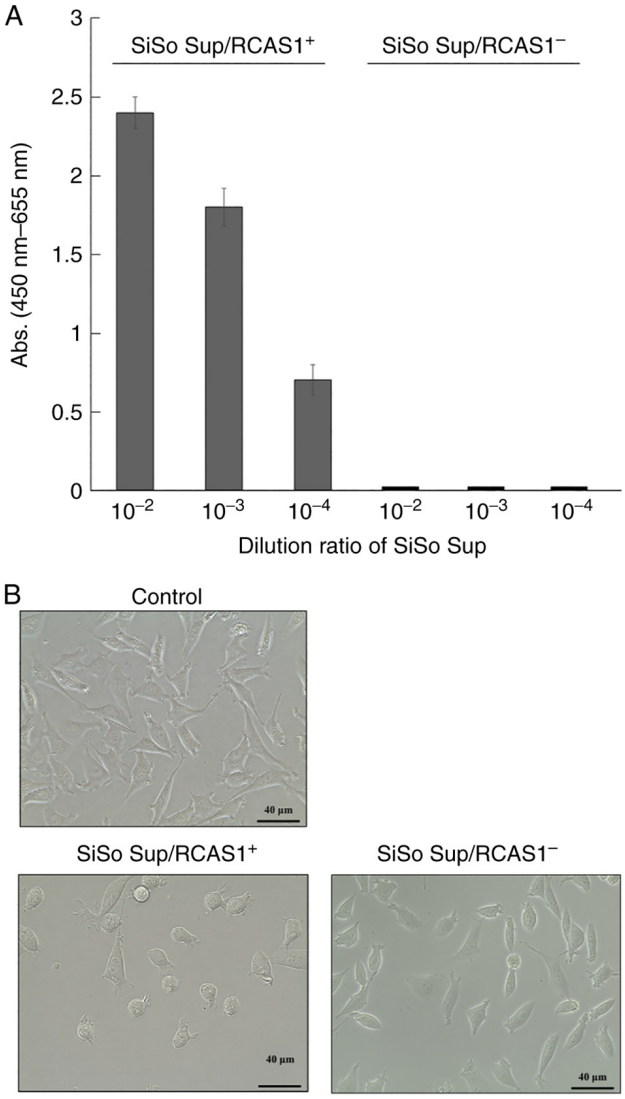

Figure 1. The effect of soluble-form RCAS1 on wild-type L cells. (A) Detection of soluble-form RCAS1 in concentrated SiSo culture supernatant was measured by ELISA. SiSo Sup/RCAS1$^+$: serum-free concentrated SiSo culture supernatant; SiSo Sup/RCAS1$^-$: fraction of SiSo Sup/RCAS1$^+$ with RCAS1 immunodepletion. (B) Observation of morphological changes in cells stimulated with SiSo Sup/RCAS1$^+$ or SiSo Sup/RCAS1$^-$; scale bar, 40 μm. RCAS1, Receptor-binding cancer antigen expressed on SiSo cells.

RCAS1 expression (Fig. 2C). These results suggested that RCAS1 expression might induce morphological changes in L/ind RCAS1 cells including the disappearance of actin stress fibers. To quantify the cell morphology, CI was analyzed by RTCA system. The CI measurement provides quantitative information about the biological status of adherent cells. In fact, the meaning of CI is the number of survival cell on the surface of E-plate. These data include the cell number, viability and morphology as a real-time profile. RTCA system showed that the CI of Dox treated cells was lower than control cells (Fig. 2D).

Effect of RCAS1 expression on the F/G-actin ratio and cofilin phosphorylation. To confirm the disappearance of actin stress fibers in L/ind RCAS1 cells, actin dynamics were examined by measuring the F/G-actin ratio and cofilin phosphorylation in L/ind RCAS1 cells. The F/G-actin ratio was significantly decreased to ~50% of the level in control cells at 6 h post-induction (Fig. 3A). On the other hand, the total amount of actin was unchanged. Subsequently, it was determined that cofilin phosphorylation, which binds to actin and regulates its polymerization and depolymerization, was significantly decreased in a time-dependent manner following Dox stimulation (Fig. 3B). These results suggested that the disappearance of actin stress fibers following RCAS1 expression might be due to increased actin depolymerization by cofilin.

Effect of RCAS1 expression on MAPK phosphorylation. MAPK signaling is upstream of the cofilin phosphorylation pathway. To examine the effect of RCAS1 on MAPK expression and phosphorylation, western blotting analysis we performed, which revealed that p38 MAPK phosphorylation was significantly decreased and in a time-dependent manner following RCAS1 expression (Fig. 4A). By contrast, ERK1/2 expression and phosphorylation were unchanged by RCAS1 expression (Fig. 4B). Decreased p38 phosphorylation was observed almost at the same time that RCAS1 expression was induced (Fig. 4A), suggesting that p38 might be closely involved in the RCAS1 signaling pathway.

Discussion

RCAS1 is expressed on the cell surface and in the cytoplasm of various cancer cells. It has been reported that soluble-form RCAS1 secreted from tumor cells acts as a ligand for a putative RCAS1 receptor (RCAS1-R) and induces cell growth inhibition and apoptosis (19). Immune cells such as T and B lymphocytes and NK cells express RCAS1-R and undergo cell growth inhibition and apoptosis following RCAS1 stimulation (19). Therefore, RCAS1 expression is thought to be related to tumor evasion from the immunosurveillance and it has been suggested that RCAS1 may serve an important role in tumor malignancy. In fact, RCAS1 expression is related to malignant characteristics, such as tumor size, invasion depth, clinical stage and poor overall survival. Thus, a number of clinical studies have reported the clinical importance of RCAS1 (20-26). By contrast, there have been few basic studies of the biological functions of RCAS1.

In the present study, it was shown that cell morphological changes (rounded shape) of L cells were observed after incubation with SiSo Sup/RCAS1+. By contrast, the cell morphological changes were not induced by SiSo Sup/RCAS1-. These results suggested that the cell morphological changes induced in L cells by SiSo Sup required RCAS1. However, the concentration of soluble-form RCAS1 was unknown in the present study. Therefore, it is planned to confirm the relationship between soluble-form RCAS1 and cell morphological changes by conducting studies using the recombinant RCAS1 protein.

Next, L/ind RCAS1 cells were used to investigate the biological functions of RCAS1. The initial results showed that cell morphological changes were observed 8 h following Dox induction. Our previous study showed that caspase-3 activation, which is a hallmark of apoptosis, was observed at 12 h following Dox induction (27). In cells undergoing apoptosis, loss of adhesion and cell morphological changes are often observed via the activated caspase cascade (32-35). However, loss of adhesion and subsequent cell detachment accompanied

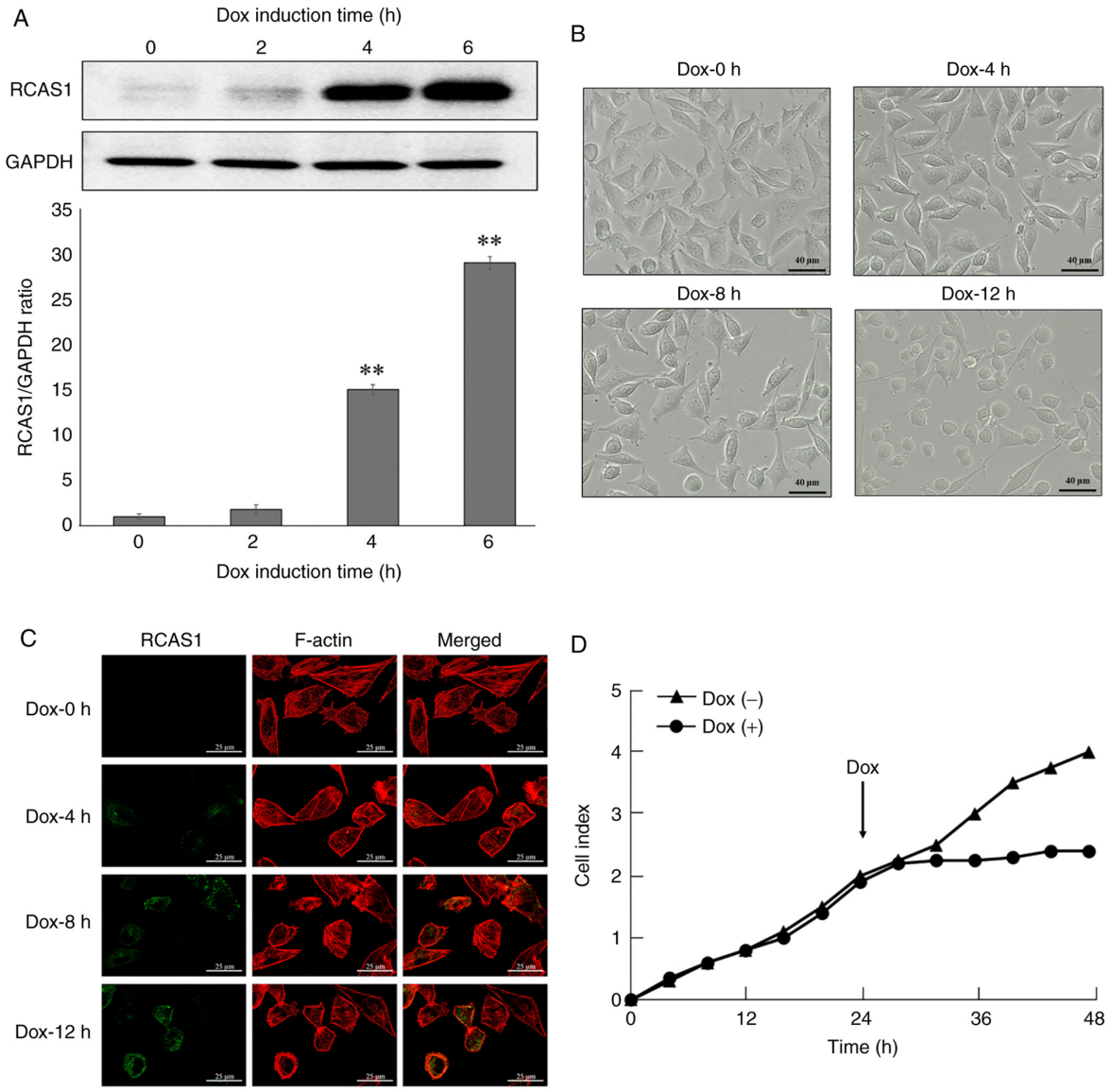

Figure 2. Effect of RCAS1 expression on the morphology of L/ind RCAS1 cells. (A) Western blot analysis of RCAS1 expression in L/ind RCAS1 cells after Dox induction. Results are presented as the mean ± standard deviation of three independent experiments; **P<0.01 vs. Dox-0 h. (B) Observations of cell morphologies induced by RCAS1; scale bar, 40 μm. (C) Effect of RCAS1 expression on actin stress fibers (F-actin) in L/ind RCAS1 cells. RCAS1 (green) was detected with an anti-RCAS1 antibody and FITC-conjugated goat-anti mouse IgG. F-actin (red) was stained with rhodamine phalloidin; scale bar, 25 μm. (D) Cell index measurement by RTCA system. RCAS1, Receptor-binding cancer antigen expressed on SiSo cells; Dox, doxycycline; RTCA, real-time cell-monitoring analysis.

by cell morphological changes can cause cell cycle arrest and a form of apoptosis termed anoikis (36-39). This suggests that apoptosis is not the trigger for RCAS1-induced cell morphological changes.

To uncover the mechanism through which RCAS1 induces cell morphological changes, the actin cytoskeleton was analyzed in L/ind RCAS1 cells. Actin is one of the major cytoskeletal proteins in eukaryotic cells and exists in cells in two forms, the globular (G-actin) and filamentous (F-actin) forms. F-actin is formed by polymerization of G-actin and the relative F/G-actin ratio is determined by the amounts of monomeric actin. F-actin is the major component of the actin cytoskeleton and critical for various cellular functions including the maintenance and regulation of cell morphology, adhesion, motility and intracellular and extracellular networks (40,41). In the present study, cytoskeleton imaging showed that actin stress fibers had disappeared together with increased RCAS1 expression. To support this finding, the F-/G-actin ratio was decreased in time-dependent following Dox induction. The polymerization or depolymerization of actin is regulated by various molecules. Cofilin is known to be a central regulator of actin dynamics that induces actin depolymerization and is inactivated by phosphorylation of serine 3 (42). Thus, the phosphorylation state of cofilin following RCAS1 expression was examined. As a result, cofilin phosphorylation was found to be significantly decreased at 6 h of Dox induction. These results suggested that the cell morphological changes induced by RCAS1 might be due to increased actin depolymerization by cofilin. Since the relationship between p38 MAP kinase and actin is more widely known (43,44), the present study focused on the analysis of actin dynamics. Meanwhile, it is clear that myosin is also involved in cell morphological changes. Therefore, the relationship between RCAS1 expression and myosin network will be analyzed in the future.

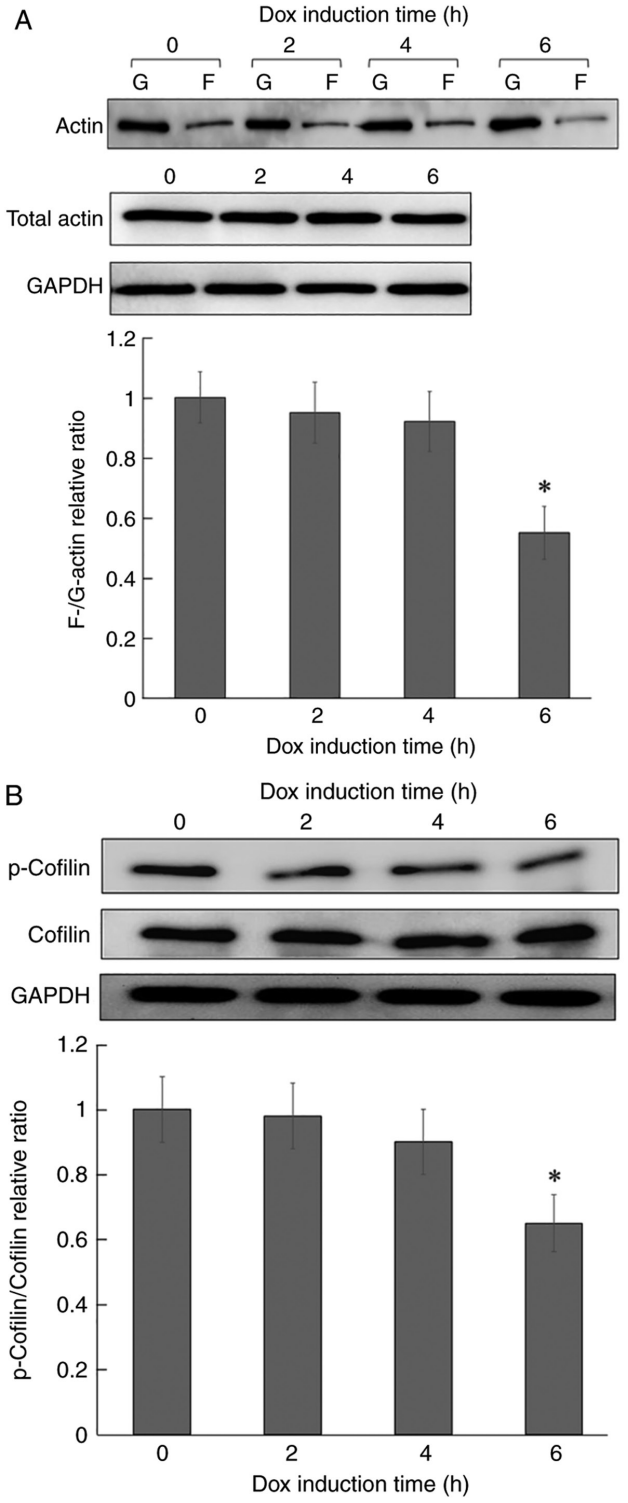

Figure 3. Effect of RCAS1 expression on actin polymerization in L/ind RCAS1 cells. (A) F- and G-actin from L/ind RCAS1 cells were separated by ultracentrifugation and determined by western blotting. (B) Analysis of cofilin phosphorylation by western blotting in L/ind RCAS1 cells after Dox induction. Results are presented as the mean ± standard deviation of three independent experiments; *P<0.05 vs. Dox -0 h. RCAS1, Receptor-binding cancer antigen expressed on SiSo cells; G, G-actin; F, F-actin; Dox, doxycycline; p-, phosphorylated.

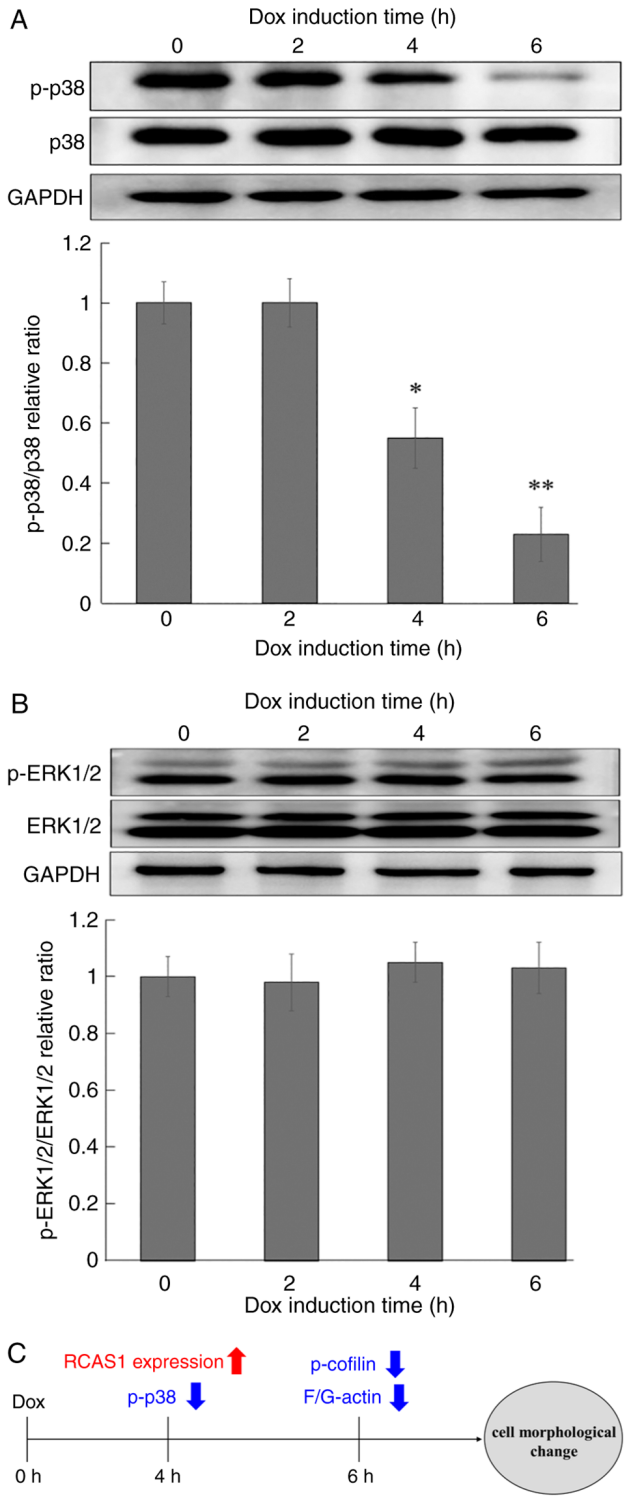

Figure 4. Effect of RCAS1 expression on MAPKs in L/ind RCAS1 cells. The amounts and phosphorylation status of (A) p38 and (B) ERK1/2 were analyzed by western blotting. (C) Time-dependent change of intracellular molecules following RCAS1 expression in L/ind RCAS1. The results are presented as the mean ± standard deviation of three independent experiments; *P<0.05 vs. Dox -0 h; **P<0.01 vs. Dox -0 h. RCAS1, Receptor-binding cancer antigen expressed on SiSo cells; Dox, doxycycline; G, G-actin; F, F-actin.

To further analyze the RCAS1 signaling pathway, the effect of RCAS1 on MAPKs we examined. The MAPK family can be divided into three groups: Jun N-terminus kinase (JNK), ERK and p38. MAPKs serve well-known roles in cell proliferation, differentiation, oncogenesis, cell death and inflammation in eukaryotes (43,44). Studies have shown that p38 signaling is connected with actin polymerization. It is reported that VEGF-A induces actin reorganization

and migration of endothelial cells through a p38 MAPK pathway (45). The p38 signaling pathway might regulate cytoskeleton rearrangements in LPS-induced macrophages (46). The present study showed that RCAS1 expression significantly decreased p38 phosphorylation levels. Markedly, the downregulation of p38 phosphorylation was detected at 4 h of Dox induction. This decrease in p38 phosphorylation was observed almost simultaneously with RCAS1 expression, suggesting that p38 might be a key molecule in the RCAS1 signaling pathway (Fig. 4C).

It is well known that p38 phosphorylation is controlled by MAP 2K and MAP 3K. To clarify the RCAS1 signal pathway, the association between RCAS1 expression and intracellular changes of MAP 2K and MAP 3K will be examined in the future. Also, in RCAS1 signal pathway, the relationship between p38 and actin dynamics remains to be elucidated. LIM kinases are regulated by several upstream signaling pathways to influence the architecture of the actin cytoskeleton by regulating the activity of the cofilin family. The p38 signal pathway is widely known as one of the upstream signals that regulate the activation of LIM kinase (45). Thus, the relationship p38 and LIM kinases in L/ind RCAS1 needs to be clarified in the future. In addition, fibroblast not tumor cells were used in this study. To clarify the RCAS1 function in tumor cells, it is necessary to investigate using tumor cells. It is planned to perform RCAS1 knockdown experiments using SiSo (human uterine carcinoma cell line) and MCF-7 (human breast cancer cells) which express RCAS1 originally. The effect of RCAS1 siRNA on intracellular molecular change in these cells will be investigated in the future.

In conclusion, the present study showed that RCAS1 expression induced a downregulation of p38 phosphorylation, followed by cytoskeletal rearrangements. Several studies have shown that molecules linked to migration signals and the cytoskeleton are upregulated in invasive and metastatic tumor cells (28,41). Additionally, it has been suggested that the p38 signaling pathway is involved not only in proliferation, metastasis and migration, but also in poor response to chemotherapy (47-49). It is hoped that the findings of the present study will contribute to the analysis of the biological functions of RCAS1 and can be applied to future tumor treatments that target RCAS1.

Acknowledgements

The authors would like to thank Professor Tomoyo Kawakubo-Yasukochi (OBT Research Center, Faculty of Dental Science, Kyushu University, Fukuoka, Japan) and Dr Manabu Nakashima (formerly of the Department of Immunological and Molecular Pharmacology, Faculty of Pharmaceutical Sciences, Fukuoka University, Fukuoka, Japan) for technical assistance and valuable discussions of the present study.

Funding

The present study was supported by JSPS KAKENHI grant number JP19K07764.

Availability of data and materials

The datasets used and/or analyzed during the current study are available from the corresponding author on reasonable request.

Authors' contributions

TN and MHa designed the project, performed the experiments, analyzed the data and prepared the manuscript. TN and MHa confirm the authenticity of all the raw data. MHo and DI designed the project. DI reviewed and edited the manuscript. All authors read and approved the manuscript.

Ethics approval and consent to participate

Not applicable.

Patient consent for publication

Not applicable.

Competing interests

The authors declare that they have no competing interests.

References

1. Fontana A, Frei K, Bodmer S, Hofer E, Schreier MH, Palladino MA Jr and Zinkernagel RM: Transforming growth factor-beta inhibits the generation of cytotoxic T cells in virus-infected mice. J Immunol 143: 3230-3234, 1989.
2. Li MO, Wan YY, Sanjabi S, Robertson AK and Flavell RA: Transforming growth factor-beta regulation of immune responses. Annu Rev Immunol 24: 99-146, 2006.
3. Kriegel MA, Li MO, Sanjabi S, Wan YY and Flavell RA: Transforming growth factor-beta: Recent advances on its role in immune tolerance. Curr Rheumatol Rep 8: 138-144, 2006.
4. Pisa P, Halapi E, Pisa EK, Gerdin E, Hising C, Bucht A, Gerdin B and Kiessling R: Selective expression of interleukin 10, interferon gamma, and granulocyte-macrophage colony-stimulating factor in ovarian cancer biopsies. Proc Natl Acad Sci USA 89: 7708-7712, 1992.
5. De Smedt T, Van Mechelen M, De Becker G, Urbain J, Leo O and Moser M: Effect of interleukin-10 on dendritic cell maturation and function. Eur J Immunol 27: 1229-1235, 1997.
6. Reed JC: Apoptosis-targeted therapies for cancer. Cancer Cell 3: 17-22, 2003.
7. Andreola G, Rivoltini L, Castelli C, Huber V, Perego P, Deho P, Squarcina P, Accomero P, Lozupone P, Lugini L, *et al*: Induction of lymphocyte apoptosis by tumor cell secretion of FasL-bearing microvesicles. J Exp Med 195: 1303-1316, 2002.
8. Okada K, Komuta K, Hashimoto S, Matsuzaki S, Kanematsu T and Koji T: Frequency of apoptosis of tumor-infiltrating lymphocytes induced by fas counterattack in human colorectal carcinoma and its correlation with prognosis. Clin Cancer Res 6: 3560-3564, 2000.
9. Reimer T, Herrnring C, Koczan D, Richter D, Gerber B, Kabelitz D, Friese K and Thiesen HJ: FasL:Fas ratio-a prognostic factor in breast carcinomas. Cancer Res 60: 822-828, 2002.
10. Bennett MW, O'Connell J, O'Sullivan GC, Brady C, Roche D, Collins JK and Shanahan F: The Fas counterattack in vivo: Apoptotic depletion of tumor-infiltrating lymphocytes associated with Fas ligand expression by human esophageal carcinoma. J Immunol 160: 5669-5675, 1998.
11. O'Connell J, Bennett MW, O'Sullivan GC, Collins JK and Shanahan F: The Fas counterattack: Cancer as a site of immune privilege. Immunol Today 120: 46-52, 1999.
12. Rivoltini L, Carrabba M, Huber V, Castelli C, Novellino L, Dalerba P, Mortarini R, Arancia G, Anichini A, Fais S and Parmiani G: Immunity to cancer: Attack and escape in T lymphocyte-tumor cell interaction. Immunol Rev 188: 97-113, 2002.
13. Huber V, Fais S, Iero M, Lugini L, Canese P, Squarcina P, Zaccheddu A, Colone M, Arancia G, Gentile M, *et al*: Human colorectal cancer cells induce T-cell death through release of proapoptotic microvesicles: Role in immune escape. Gastroenterology 128: 1796-1804, 2005.

14. Giovarelli M, Musiani P, Garotta G, Ebner R, Di Carlo E, Kim Y, Cappello P, Rigamonti L, Bernabei P, Novelli F, *et al*: A 'stealth effect': Adenocarcinoma cells engineered to express TRAIL elude tumor-specific and allogeneic T cell reactions. J Immunol 163: 4886-4893, 1999.
15. Koyama S, Koike N and Adachi S: Expression of TNF-related apoptosis-inducing ligand (TRAIL) and its receptors in gastric carcinoma and tumor-infiltrating lymphocytes: A possible mechanism of immune evasion of the tumor. J Cancer Res Clin Oncol 128: 73-79, 2002.
16. Kassouf N and Thornhill MH: Oral cancer cell lines can use multiple ligands, including Fas-L, TRAIL and TNF-alpha, to induce apoptosis in Jurkat T cells: Possible mechanisms for immune escape by head and neck cancers. Oral Oncol 44: 672-682, 2008.
17. Sonoda K, Nakashima M, Saito T, Amada S, Kamura T, Nakano H and Watanabe T: Establishment of a new human uterine cervical adenocarcinoma cell-line, siso, and its reactivity to anticancer reagents. Int J Oncol 6: 1099-1104, 1995.
18. Sonoda K, Nakashima M, Kaku T, Kamura T, Nakano H and Watanabe T: A novel tumor-associated antigen expressed in human uterine and ovarian carcinomas. Cancer 77: 1501-1509, 1996.
19. Nakashima M, Sonoda K and Watanabe T: Inhibition of cell growth and induction of apoptotic cell death by the human tumor-associated antigen RCAS1. Nat Med 5: 938-942, 1999.
20. Enjoji M, Nakamuta M, Noguchi K, Sugimoto R, Kotoh K, Nawata H, Nakashima M and Watanabe T: RCAS1 expression in immune-mediated liver diseases. J Clin Gastroenterol 34: 286-287, 2002.
21. Enjoji M, Nakashima M, Yamaguchi K, Kotoh K and Nakamuta M: Significance of RCAS1 antigen in hepatocellular, cholangiocellular and pancreatic carcinomas. J Gastroenterol Hepatol 20: 1143-1148, 2005.
22. Giaginis C, Giagini A and Theocharis S: Receptor-binding cancer antigen expressed on SiSo cells (RCAS1): A novel biomarker in the diagnosis and prognosis of human neoplasia. Histol Histopathol 24: 761-776, 2009.
23. Dutsch-Wicherek M: RCAS1, MT, and vimentin as potential markers of tumor microenvironment remodeling. Am J Reprod Immunol 63: 181-188, 2010.
24. Sonoda K: Novel therapeutic strategies to target RCAS1, which induces apoptosis via ectodomain shedding. Histol Histopathol 26: 1475-1486, 2011.
25. Szubert S, Dziobek K and Wicherek L: High post-treatment serum soluble receptor-binding cancer antigen expressed on SiSo cells (sRCAS1) levels is associated with poor survival of patients with cervical cancer. J Obset Gynaecol Res 46: 499-506, 2020.
26. Sonoda K, Miyamoto S, Nakashima M and Wake N: Receptor-binding cancer antigen expressed on SiSo cells induces apoptosis via ectodomain shedding. Exp Cell Res 316: 1795-1803, 2010.
27. Nishinakagawa T, Fujii S, Nozaki T, Maeda T, Machida K, Enjoji M and Nakashima M: Analysis of cell cycle arrest and apoptosis induced by RCAS1. Int J Mol Med 25: 717-722, 2010.
28. Yamaguchi H and Condeelis J: Regulation of the actin cytoskeleton in cancer cell migration and invasion. Biochim Biophys Acta 1773: 642-652, 2007.
29. Condeelis J, Singer R and Segall JE: The great escape: When cancer cells hijack the genes for chemotaxis and motility. Annu Rev Cell Dev Biol 21: 695-718, 2005.
30. Sahai E: Mechanisms of cancer cell invasion. Curr Opin Genet Dev 15: 87-96, 2005.
31. Yamaguchi H, Wyckoff J and Condeelis J: Cell migration in tumors. Curr Opin Cell Biol 17: 559-564, 2005.
32. Kim B, van Golen CM and Feldman EL: Insulin-like growth factor I induces preferential degradation of insulin receptor substrate-2 through the phosphatidylinositol 3-kinase pathway in human neuroblastoma cells. Endocrinology 146: 5350-5357, 2005.
33. Lavastre V, Chiasson S, Cavalli H and Girard D: Viscum album agglutinin-I induces apoptosis and degradation of cytoskeletal proteins via caspases in human leukaemia eosinophil AML14.3D10 cells: Differences with purified human eosinophils. Br J Haematol 130: 527-535, 2005.
34. Lavastre V, Pelletier M, Saller R, Hostanska K and Girard D: Mechanisms involved in spontaneous and Viscum album agglutinin-I-induced human neutrophil apoptosis: Viscum album agglutinin-I accelerates the loss of antiapoptotic Mcl-1 expression and the degradation of cytoskeletal paxillin and vimentin proteins via caspases. J Immunol 168: 1419-1427, 2002.
35. Levkau B, Herren B, Koyama H, Ross R and Raines EW: Caspase-mediated cleavage of focal adhesion kinase pp125FAK and disassembly of focal adhesions in human endothelial cell apoptosis. J Exp Med 187: 579-586, 1998.
36. Frisch SM and Francis H: Disruption of epithelial cell-matrix interactions induces apoptosis. J Cell Biol 124: 619-626, 1994.
37. Frisch SM, Vuori K, Ruoslahti E and Chan-Hui PY: Control of adhesion-dependent cell survival by focal adhesion kinase. J Cell Biol 134: 793-799, 1996.
38. Wu WB, Peng HC and Huang TF: Disintegrin causes proteolysis of beta-catenin and apoptosis of endothelial cells. Involvement of cell-cell and cell-ECM interactions in regulating cell viability. Exp Cell Res 286: 115-127, 2003.
39. Zhao JH, Reiske H and Guan JL: Regulation of the cell cycle by focal adhesion kinase. J Cell Biol 143: 1997-2008, 1998.
40. Milligan RA, Whittaker D and Safer D: Molecular structure of F-actin and location of surface binding sites. Nature 348: 217-221, 1990.
41. Dos Remedios CG, Chhabra D, Kekic M, Dedova IV, Tsubakihara M, Berry DA and Nosworthy NJ: Actin binding proteins: Regulation of cytoskeletal microfilaments. Physiol Rev 83: 433-473, 2003.
42. Moon A and Drubin DG: The ADF/cofilin proteins: Stimulus-responsive modulators of actin dynamics. Mol Biol Cell 6: 1423-1431, 1995.
43. Qi M and Elion EA: MAP kinase pathways. J Cell Sci 118: 3569-3572, 2005.
44. Johnson GL and Lapadat R: Mitogen-activated protein kinase pathways mediated by ERK, JNK, and p38 protein kinases. Science 298: 1911-1912, 2002.
45. Kobayashi M, Nishita M, Mishima T, Ohashi K and Mizuno K: MAPKAPK-2-mediated LIM-kinase activation is critical for VEGF-induced actin remodeling and cell migration. EMBO J 25: 713-726, 2006.
46. Bian H, Li F, Wang W, Zhao Q, Gao S, Ma J, Li X, Ren W, Qin C and Qi J: MAPK/p38 regulation of cytoskeleton rearrangement accelerates induction of macrophage activation by TLR4, but not TLR3. Int J Mol Med 40: 1495-1503, 2017.
47. Koul HK, Pal M and Koul S: Role of p38 MAP kinase signal transduction in solid tumors. Genes Cancer 4: 342-359, 2013.
48. Pereira L, Igea A, Canovas B, Dolado I and Nebreda AR. Inhibition of p38 MAPK sensitizes tumour cells to cisplatin-induced apoptosis mediated by reactive oxygen species and JNK. EMBO Mol Med 5: 1759-1774, 2013.
49. Bakour N, Moriarty F, Moore G, Robson T and Annett SL: Prognostic significance of glucocorticoid receptor expression in cancer: A systematic review and meta-analysis. Cancers (Basel) 13: 1649, 2021.